Angewandte Chemie
Eine Zeitschrift der Gesellschaft Deutscher Chemiker

Supporting Information

Site-Specific Hyperphosphorylation Inhibits, Rather than Promotes, Tau Fibrillization, Seeding Capacity, and Its Microtubule Binding**

*Mahmood Haj-Yahya, Pushparathinam Gopinath[+], Kolla Rajasekhar[+], Hilda Mirbaha, Marc I. Diamond, and Hilal A. Lashuel**

anie_201913001_sm_miscellaneous_information.pdf

Supporting Information

Synthesis of tau(322-372)-$CONH_2$ (1):

Sequence:**CGSLGNIHHKPGGGQVEVKSEKLDFKDRVQSKIGSLDNITHVPGGGNKKIE**

tau (322-372) (1) was synthesized using a Rink amide-MBHA resin (0.27 mmol/g, 0.1 mmol scale) according to the following procedure: the first amino acid (AA), glutamine (Glu), was double coupled manually for 1 h (×2) using 4 eq of 1-[bis(dimethylamino)methylene]-1H-1,2,3-triazolo[4,5-b]pyridinium3- oxid hexafluorophosphate (HATU) and 8 eq of N,N-diisopropylethylamine (DIEA). The remaining AAs were double coupled using an automated CS 336X peptide synthesizer from CS Bio and carried out by mixing 4 eq of the AA with 8 eq of DIEA and 4 eq of O-(1H-6-chlorobenzotriazole-1-yl)-1,1,3,3-tetramethyluronium hexafluorophosphate (HCTU) in N-methyl 2-pyrrolidone (NMP). Each coupling reacted for 45 min, and Fmoc deprotection was achieved using 20% piperidine and 50 mM 1-hydroxybenzotriazole hydrate (HOBt) in 3/5/3 min cycles. The last AA, cysteine (Cys), was introduced with N-terminal Boc protection.

Cleavage from the resin: Once the synthesis was complete, the resin was washed with dimethylformamide (DMF), methanol, and DCM, and the dried peptidyl-resin was treated with a cleavage cocktail containing 95% trifluoroacetic acid (TFA), 2.5% water, and 2.5% triisopropylsilane (TIPS) for 2.5 h at room temperature (RT). The crude peptide was then precipitated by the dropwise addition of a 10-fold volume of cold ether and centrifuged. The pellet was dissolved in 30-50% aqueous acetonitrile and lyophilized. The crude peptide was then purified by RP-HPLC using a preparative C18 column with a linear gradient of 30-60% B over 40 min, resulting in a 25% yield of the final peptide (Figure S1).

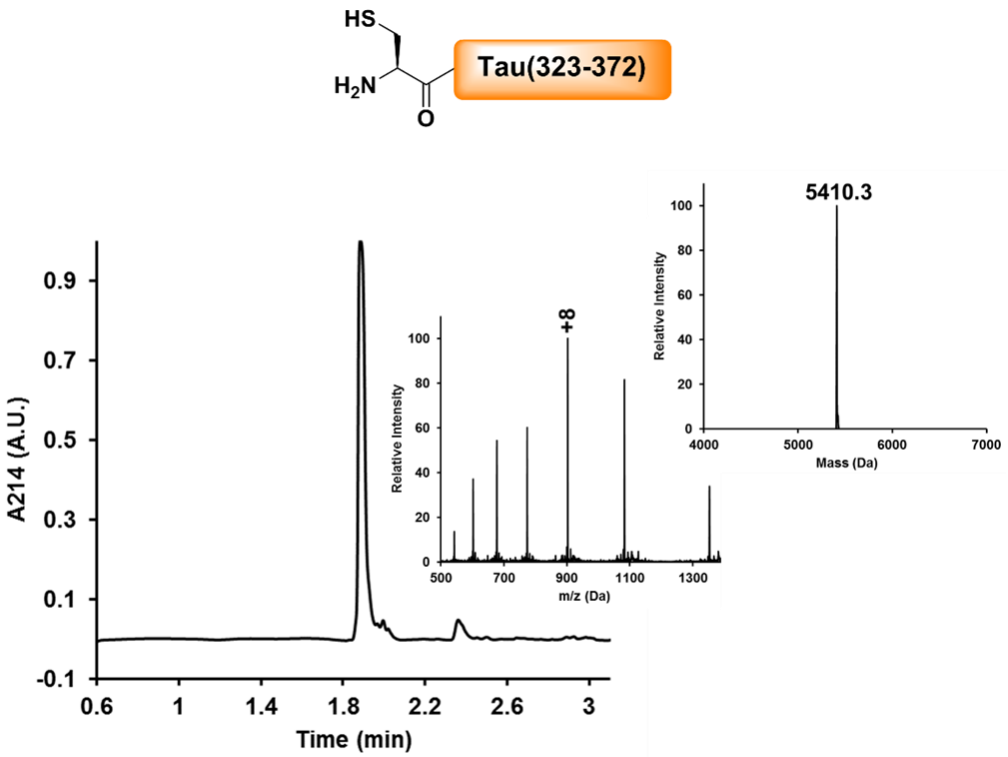

Figure S1. SPPS of tau (322-372). Analytical RP-UHPLC and ESI-MS of the purified peptide **1**, with the observed mass of 5410.3 Da (calculated 5409.13 Da).

Synthesis of tau(322-372, pS356)-CONH$_2$ (1a):

Sequence:**CGSLGNIHHKPGGGQVEVKSEKLDFKDRVQSKIGpSLDNITHVPGGGNKKIE**

tau (322-272, pS356)-CONH$_2$ (1a) was prepared as described for peptide **1**, with the following modifications: 2.5 eq of Fmoc-Ser(HPO$_3$Bzl)-OH was coupled at position 356 for 2 h. Additionally, 2.5 eq of the pseudoproline dipeptide of Ile-Thr were manually coupled for 2 h at position Ile360-Thr361. The lyophilized crude peptide was then purified by RP-HPLC using a preparative C18 column with a linear gradient of 30-60% B over 40 min, resulting in ~20% yield of the final peptide (Figure S2).

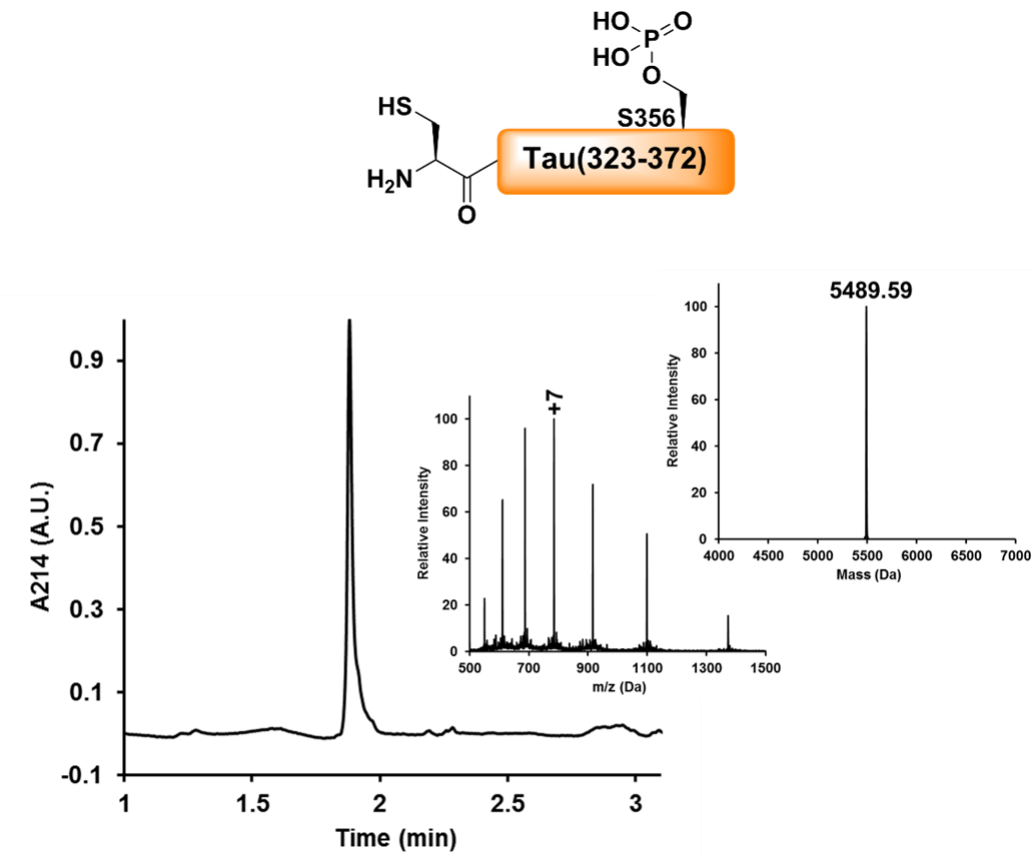

Figure S2. SPPS of tau (322-372, pS356). Analytical RP-HPLC and ESI-MS of the purified peptide **1a**, with the observed mass of 5489.59 Da (calculated 5489.10 Da).

Synthesis of tau (C291Thz-321)-SR (2):

Sequence: **Thz-GSKDNIKHVPGGGSVQIVYKPVDLSKVTSK**

tau (C291Thz-321)-SR (2) was synthesized using Rink amide-MBHA resin (0.27 mmol/g, 0.1 mmol scale) according to the following procedure: The first unnatural AA, 3-(Fmoc-amino)-4-(methylamino) benzoic acid, was double coupled manually for 1 h (×2) using 4 eq of HATU and 8 eq of DIEA. The remaining AAs were double coupled using an automated CS 336X peptide synthesizer from CS Bio and carried out in the presence of 4 eq of AA, 8 eq of DIEA and 4 eq of HCTU. Each coupling reacted for 45 min, and Fmoc deprotection was achieved using 20% piperidine and 50 mM HOBt in 3/5/3 min cycles. The last AA was introduced with N-terminal Boc protection. After peptide elongation, the resin was reswelled with dichloromethane (DCM) for 15 min and reacted with a solution of p-nitrophenyl chloroformate (5 eq in 2 ml of DCM) for 1 h at RT. Then, the resin was

washed with DCM and reswelled with DMF for 15 min. To that, a solution of 0.5 M DIEA in 1 ml of DMF was added for 15 min (×2).

Cleavage from the resin: After washing with DMF, methanol, and DCM, the dried peptidyl-resin was treated with a cleavage cocktail containing 95% TFA, 2.5% water and 2.5% TIPS for 2.5 h at RT. The crude peptide was then precipitated by the dropwise addition of a 10-fold volume of cold ether and centrifuged. The precipitate was then dissolved in 30-50% aqueous acetonitrile and lyophilized. The crude peptide was then purified by RP-HPLC using a preparative C18 column with a linear gradient of 10-40% B over 40 min, resulting in 22.5% yield of the thioester (Figure S3).

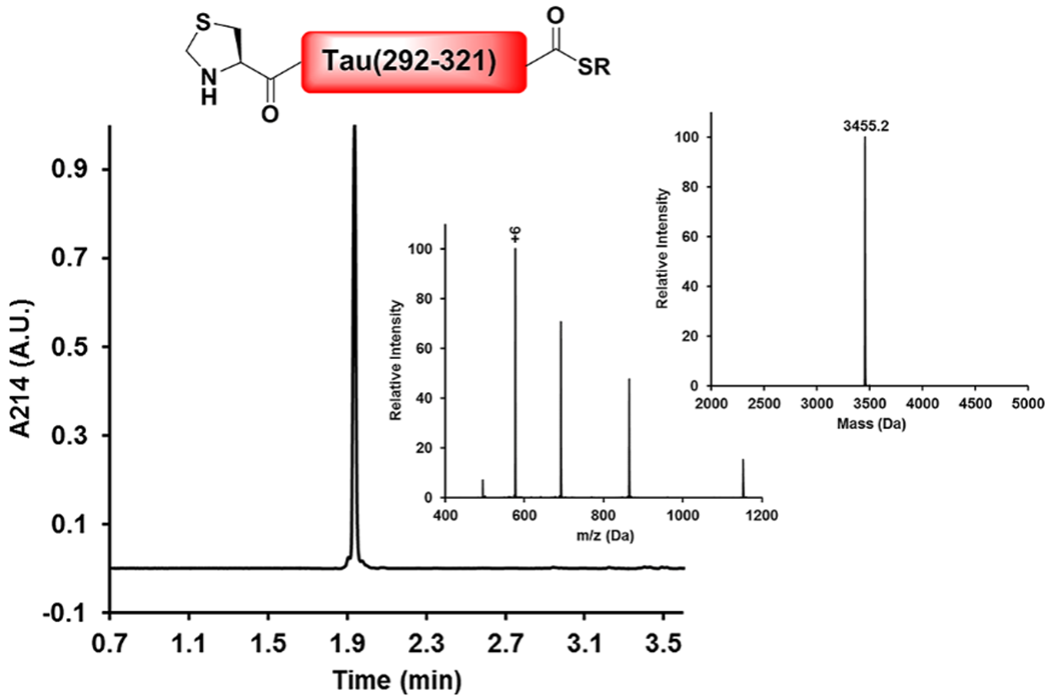

Figure S3. SPPS of tau (C291Thz-321)-SR. Analytical RP-HPLC and ESI-MS of the purified thioester **(2)**, with the observed mass of 3455.20 Da (calculated 3455.50 Da).

Synthesis of tau (243-290)-SR (3):

Sequence:

LQTAPVPMPDLKNVKSKIGSTENLKHQPGGGKVQIINKKLDLSNVQSK

tau (243-290)-SR (3) was synthesized as described above with the following modifications: 2.5 eq of the pseudoproline dipeptides of Leu-Ser was manually coupled for 2 h at the Leu284-Ser285 junction. The peptide was purified by RP-HPLC using a

preparative C18 column with a linear gradient of 30-60% B over 40 min, resulting in ~15% yield of the thioester (Figure S4).

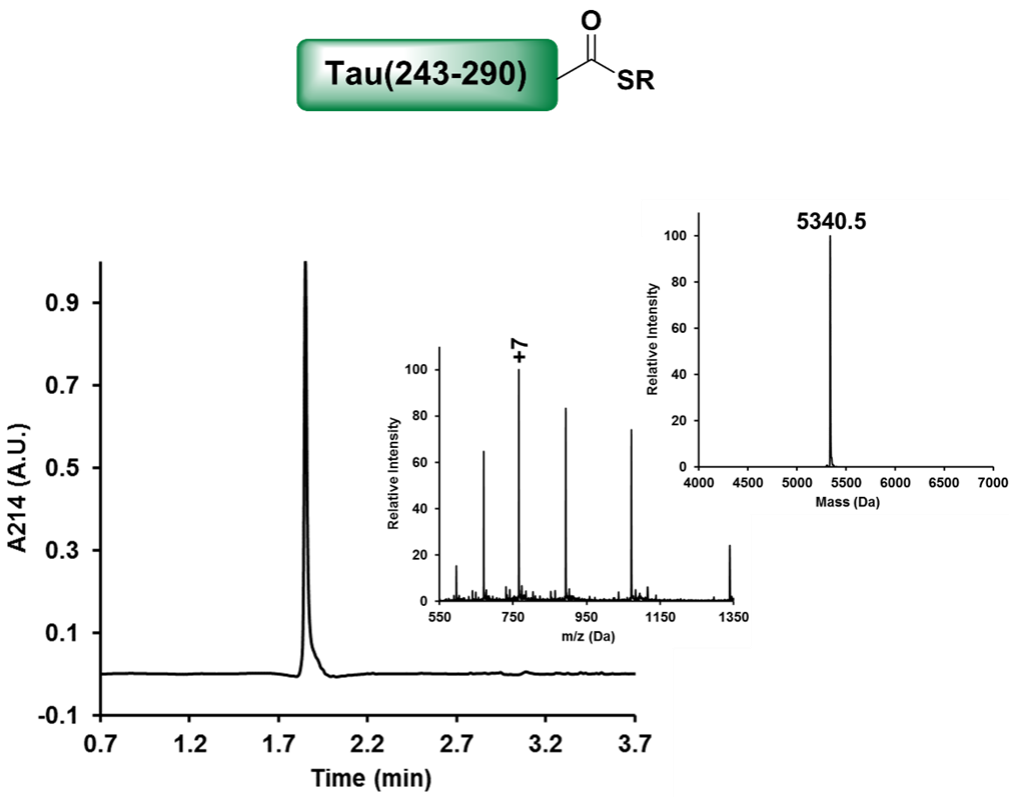

Figure S4. SPPS of tau (243-290)-SR. Analytical RP-HPLC and ESI-MS of the purified peptide **(3)**, with the observed mass of 5340.50 Da (calculated 5337.05 Da).

<u>Synthesis of tau(243-290, pS262)-SR (3a):</u>

Sequence:

LQTAPVPMPDLKNVKSKIGpSTENLKHQPGGGKVQIINKKLDLSNVQSK

tau (243-290, pS262)-SR (3a) was synthesized similarly to the WT peptide **(3)** described above with the following modification: 2.5 eq of Fmoc-Ser(HPO_3Bzl)-OH was coupled manually at position 262 for 2 h. The peptide was purified by RP-HPLC using a preparative C18 column with a linear gradient of 30-60% B over 40 min, resulting in an 8% yield of the thioester (Figure S5).

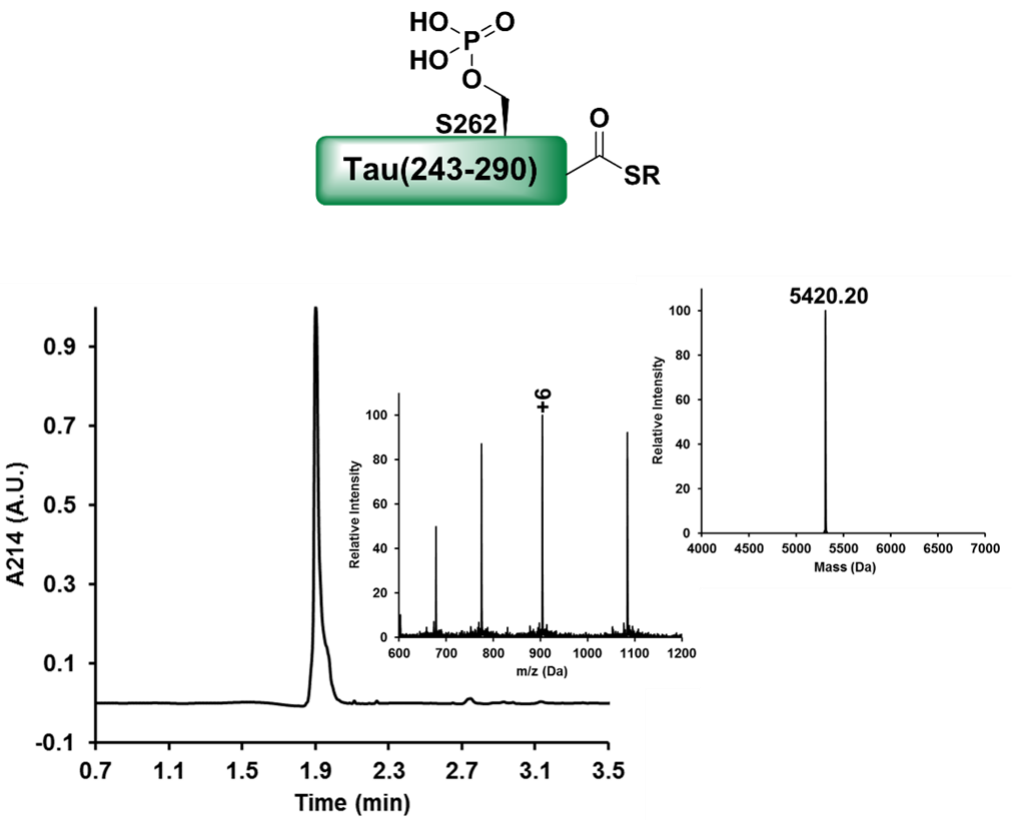

Figure S5. SPPS of tau (243-290, pS262)-SR. Analytical RP-HPLC and ESI-MS of the purified peptide **3a**, with the observed mass of 5420.20 Da (calculated 5417.05 Da).

Synthesis of tau(243-290, pS262, pS258)-SR (3b):

Sequence:

LQTAPVPMPDLKNVKpSKIGpSTENLKHQPGGGKVQIINKKLDLSNVQSK

tau (243-290, pS262, pS258)-SR (3b) was synthesized similarly to peptide **3** described above with the following changes: 2.5 eq of Fmoc-Ser(HPO_3Bzl)-OH was coupled manually at positions 262 and 258 for 2 h each. The peptide was purified by RP-HPLC using a preparative C18 column with a linear gradient of 30-60% B over 40 min, resulting in a 7.3% yield of the thioester (Figure S6).

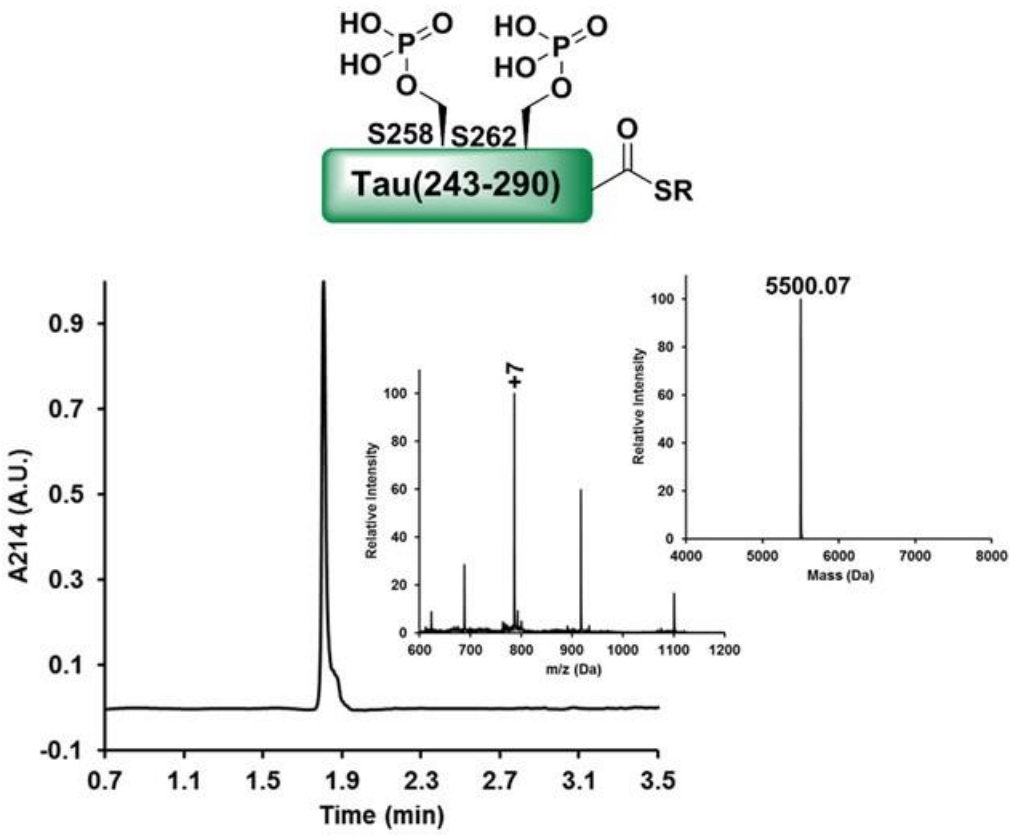

Figure S6. SPPS of tau (243-290, pS262, pS258)-SR. Analytical RP-HPLC and ESI-MS of the purified peptide **3b**, with the observed mass of 5500.07 Da (calculated 5497.05 Da).

Ligation of tau (C291Thz-321)-SR with tau (322-372):

tau (322-372) (1) (10 mg, 1 eq) and **tau (C291Thz-321)-SR (2)** (9 mg, 1.4 eq) were dissolved in ligation buffer (6 M guanidine hydrochloride (GdnHCl), 0.2 M sodium phosphate, 25 eq tris(2-carboxyethyl)phosphine (TCEP), 20 eq 4- mercaptophenylacetic acid (MPAA), pH 7.0) that had been purged with nitrogen. The mixture was incubated at 37 ºC for 4.5 h with orbital agitation at 600 rpm and monitored by RP-UHPLC and mass spectrometry analyses.

In situ thiazolidine deprotection: Upon completion of the ligation reaction, a solution of 0.2 M methoxylamine, 30 eq TCEP in a nitrogen purged 6 M GdnHCl, 0.2 M phosphate was added to the ligation mixture and then incubated at 37 °C for 12 h with orbital agitation at 600 rpm. The reaction was monitored by RP-UHPLC and mass spectrometry analyses. The ligated product was purified by RP-HPLC using a semi-preparative C4 column with a

linear gradient of 20% (30 min)-35% B over 50 min, resulting in 17.2% yield of the product **4** over two steps (Figure S7).

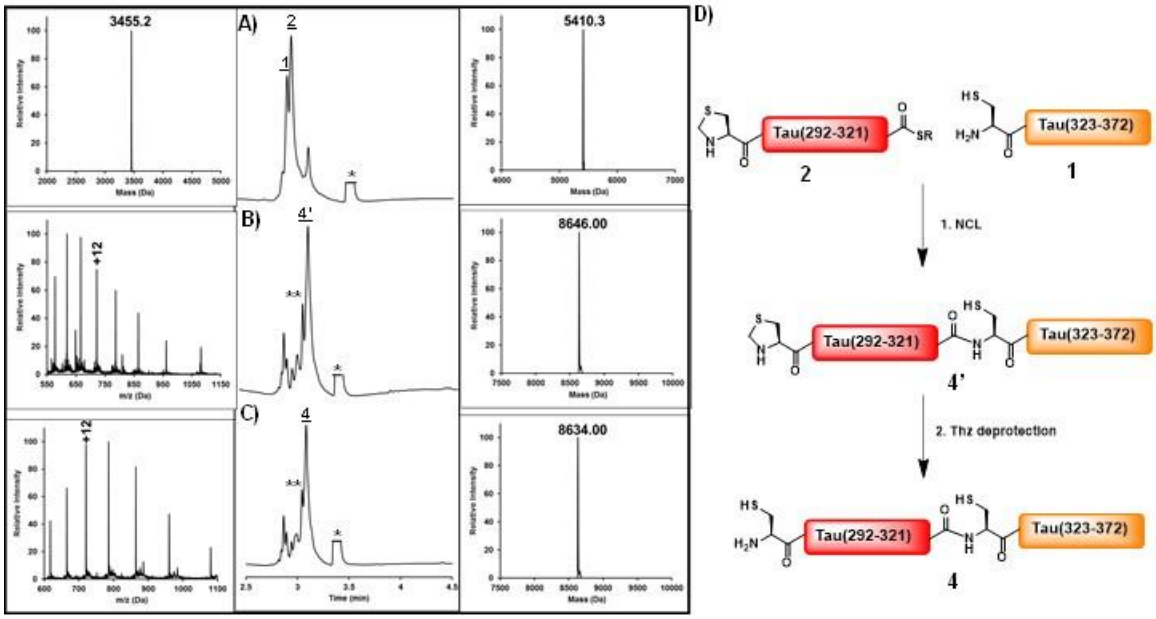

Figure S7. Native chemical ligation for the preparation of fragment 4: Analytical RP-HPLC and ESI-MS spectra of the ligation reaction between tau (322-372) and tau (C291Thz-321)-SR at A) 0 h and after B) 4.5 h. Peak **4** corresponds to the ligation product with the observed mass of 8646.00 Da (calculated 8646.00 Da). Peak ** corresponds to the hydrolyzed thioester, and peak * corresponds to the MPAA thiol. C) Analytical RP-HPLC and ESI-MS spectra of the in situ thiazolidine deprotection reaction after 12 h. Peak **4** corresponds to the product with free cysteine at the N-terminus, with the observed mass 8634.00 Da (calculated 8633.85 Da). D) Schematic representation of the NCL of the tau (291-372) fragment.

Ligation of tau (243-290)-SR with tau (291-372):

tau (291-372) (4) (3 mg, 1 eq) and **tau (243-290)-SR (3)** (2.4 mg, 1.3 eq) were dissolved in NCL purged buffer (8.0 M urea, 25 mM TCEP, 2% TFET, pH 7.0). The mixture was incubated at 37 ºC for 2 h with orbital agitation at 600 rpm and monitored by RP-UHPLC and mass spectrometry analyses. The ligated product was purified by RP-HPLC using a semipreparative C18 column with a linear gradient of 20-35% B over 50 min, resulting in 19% yield of the product **5** (Figure S8).

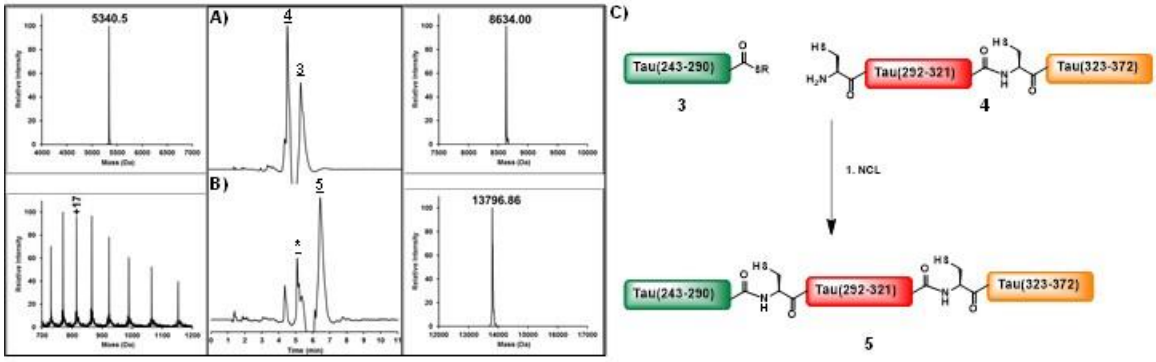

Figure S8. Native chemical ligation for the preparation of K18 (5): Analytical RP-HPLC and ESI-MS spectra of the ligation reaction between tau (243-290)-SR and tau (291-372) at A) 0 h and B) after 2 h. Peak **5** corresponds to the ligation product with the observed mass of 13796.00 Da (calculated 13795.00 Da). Peak * corresponds to the hydrolyzed thioester. C) Schematic representation of the total chemical synthesis of the tau (243-372) fragment (K18).

Preparation of monophosphorylated K18 at Ser356:

tau (322-372, pS356) (1a) (7 mg, 1 eq) and **tau (C291Thz-321)-SR (2)** (5.7 mg, 1.3 eq) were dissolved in ligation buffer (6.0 M GdnHCl, 25 mM TCEP, 2% TFET, pH 7.0). The mixture was left at 37 ºC for 1.5 h with orbital agitation at 600 rpm and monitored by RP-UHPLC and mass spectrometry.

In situ thiazolidine deprotection: Upon completion of the ligation reaction, a solution of 0.2 M methoxylamine and 30 eq of TCEP in a nitrogen purged 6.0 M GdnHCl, 0.2 M phosphate solution was added to the ligation mixture and then incubated at 37 °C for 12 h with orbital agitation at 600 rpm. The reaction was monitored by RP-UHPLC and mass spectrometry analyses. The ligated product was purified by RP-HPLC using a semi-preparative C18 column with a linear gradient of 20-35% B over 50 min, resulting in 17.2% yield of product **4a** over two steps (Figure S9).

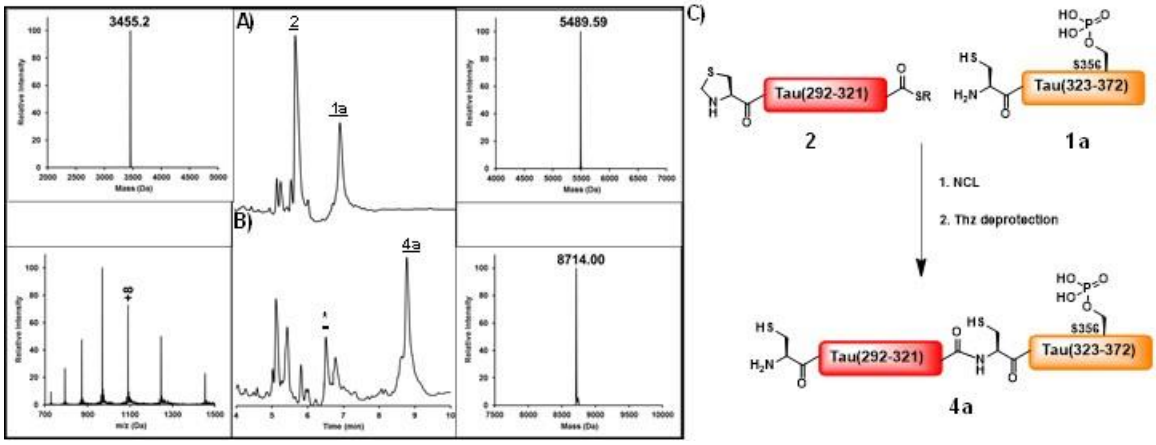

Figure S9. Native chemical ligation for the preparation of fragment 4a. Analytical RP-HPLC and ESI-MS spectra of the ligation reaction between tau (322-372, pS356) and tau (C291Thz-321)-SR at A) 0 h and B) after 1.5 h. Peak **4a** corresponds to the ligation product after Thz deprotection with the observed mass of 8714.00 Da (calculated 8713.85 Da). Peak * corresponds to the hydrolyzed thioester. C) Schematic representation of the NCL of the tau (291-372, pS356) fragment.

Ligation of tau(243-290)-SR with tau(291-372, pS356):

tau (291-372, pS356) (4a) (2.8 mg, 1 eq) and **tau (243-290)-SR (3)** (2.2 mg, 1.3 eq) were dissolved in NCL purged buffer (6.0 M GdnHCl, 25 eq TCEP, 20 eq MPAA, pH 7.0). The mixture was incubated at 37 ºC for 2 h with orbital agitation at 600 rpm and monitored by RP-UHPLC and mass spectrometry analyses. The ligated product was purified by RP-HPLC using a semipreparative C4 column with a linear gradient of 10-55% B over 55 min to afford the corresponding product **6** in 25% yield (Figure S10).

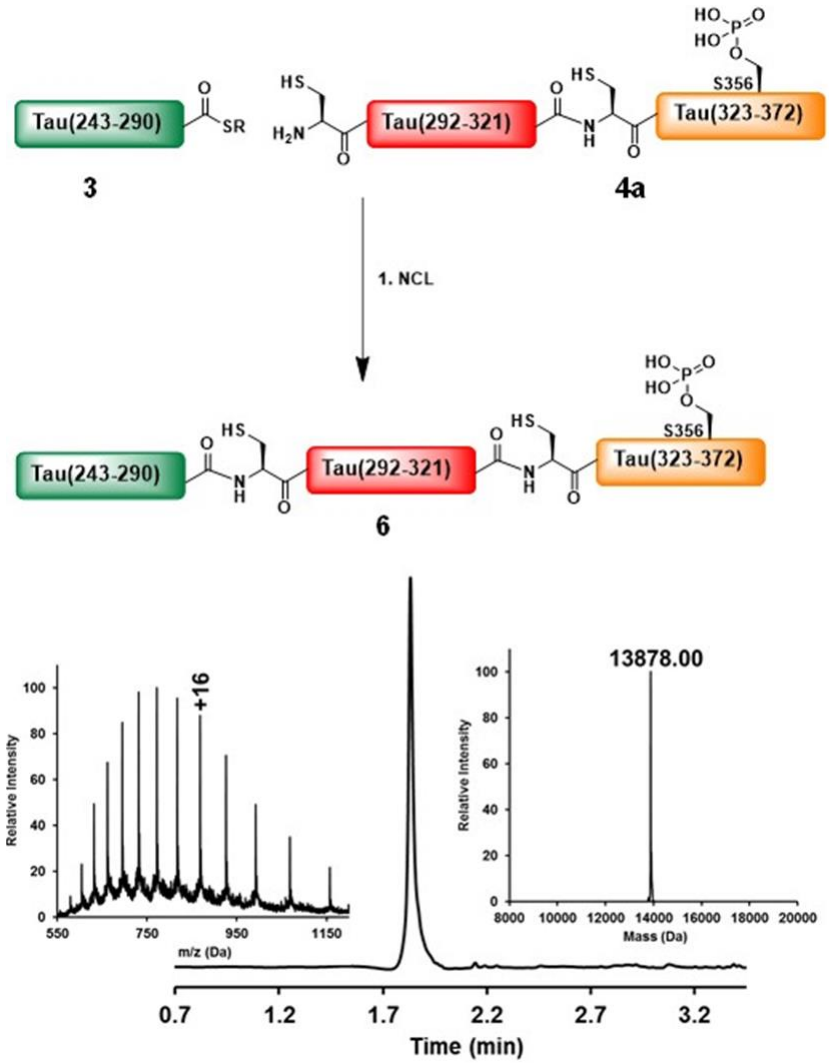

Figure S10. Native chemical ligation for the preparation of K18_pS356 (6). A) Schematic representation of the total synthesis of monophosphorylated tau (243-372, pS356) fragment (K18_pS356). B) Analytical RP-HPLC and ESI-MS spectra of K18_pS356, with the observed mass of 13878.00 Da (calculated 13875.89 Da).

Preparation of diphosphorylated K18 at Ser 356 & Ser 262:

Ligation of tau(243-290, pS262)-SR with tau(291-372, pS356):

tau (291-372, pS356) (4a) (2.3 mg, 1 eq) and **tau (243-290, pS262)-SR (3a)** (2.0 mg, 1.4 eq) were dissolved in NCL purged buffer (8.0 M urea, 50 mM TCEP, 2% TFET, pH 7.0). The mixture was incubated at 37 ºC for 3 h with orbital agitation at 600 rpm and monitored by RP-UHPLC and mass spectrometry analyses. The ligated product was purified by RP-HPLC using a semipreparative C18 column with a linear gradient of 5-23% B (20 min), 20-40% B over 50 min, resulting in a 25.5% yield of product **7** (Figure S11).

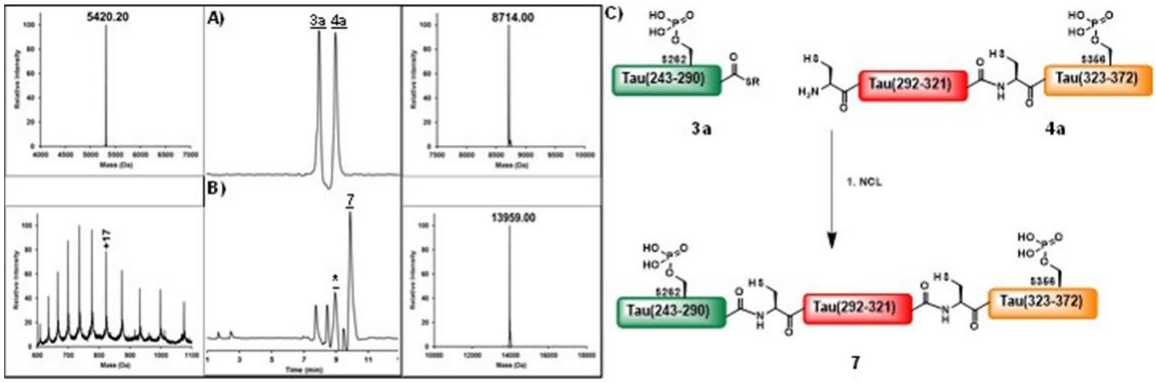

Figure S11. Native chemical ligation for the preparation of K18_pS356, pS262 (7). Analytical RP-HPLC and ESI-MS spectra of the ligation reaction between tau (291-372, pS356) and tau (243-290, pS262)-SR at A) 0 h and after B) 3 h. Peak **7** corresponds to the ligation product with the observed mass of 13959.00 Da (calculated 13955.85 Da). Peak * corresponds to the hydrolyzed thioester. C) Schematic representation of the total synthesis of diphosphorylated tau (243-372, pS356, pS262) fragment (K18_pS356, pS262).

Preparation of triphosphorylated K18 at Ser 356, Ser 262, & Ser 258:

Ligation of tau(243-290, pS262, pS258)-SR with tau(291-372, pS356):

tau (291-372, pS356) (4') (2.8 mg, 1 eq) and **tau (243-290, pS262, pS258)-SR (3b)** (4.4 mg, 2.4 eq) were dissolved in NCL purged buffer (8.0 M urea, 50 mM TCEP, 2% TFET, pH 7.0). The mixture was incubated at 37 ºC for 2 h with orbital agitation at 600 rpm and monitored by RP-UHPLC and mass spectrometry analyses. The ligated product was purified by RP-HPLC using a semipreparative C18 column with a linear gradient of 20-40% B over 40 min, resulting in a 27% yield of product **8** (Figure S12).

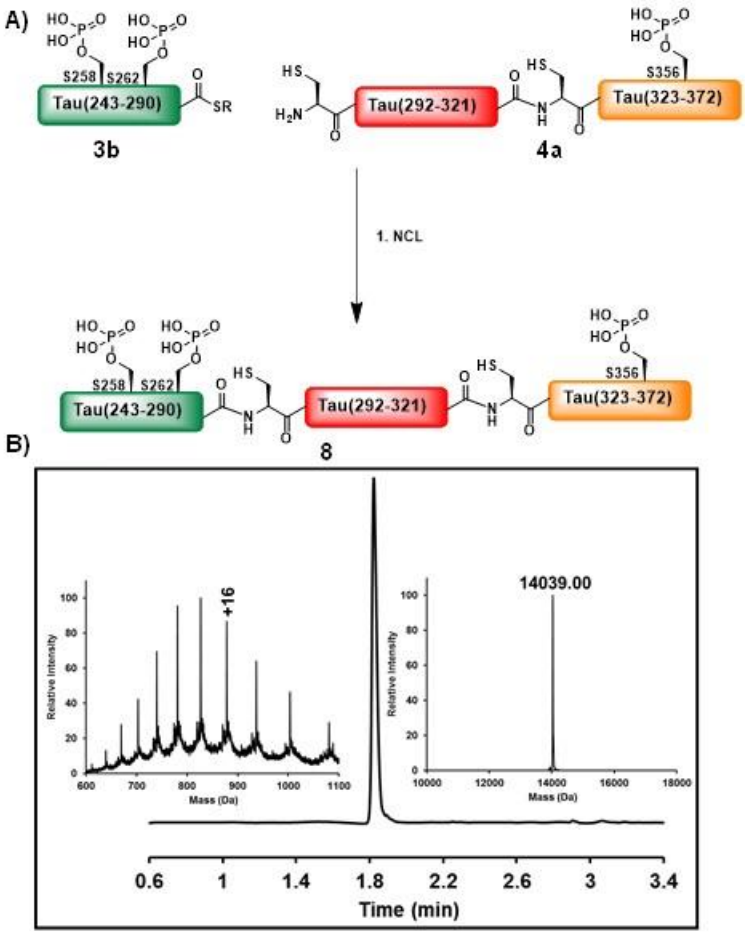

Figure S12. Native chemical ligation for the preparation of K18_pS356, pS262, pS258 (8). A) Schematic representation of the total synthesis of the triphosphorylated tau (243-372, pS356, pS262, pS258) fragment (K18_pS356, pS262, pS258). B) Analytical RP-HPLC and ESI-MS spectra of the purified K18 fragment triphosphorylated at Ser 356, Ser 262, and Ser 258, with the observed mass of 14039.00 Da (calculated 14035.89 Da).

***In vitro* phosphorylation of tyrosine 310 (Tyr 310):**

K18_pS356, pS262, pS258 (1 mg, 1 eq) was dissolved in 10% urea and subsequently diluted in 50 mM Tris.HCl (pH 7.0) containing 1 mM DTT, 5 mM $MgCl_2$, 20 mM Va_3NO_4, and 5 mM ATP for a final concentration of peptide of 1 mg/ml. The enzymatic assay was initiated by incubation of peptide **8** with c-Abl (0.7 mg, 0.2 eq) for 5 h at 30 °C without agitation. The reaction was monitored by RP-UHPLC and mass spectrometry analyses to verify the completion of phosphorylation. The phosphorylated peptide was purified by RP-HPLC using a semipreparative C18 column with a linear gradient of 20-35% B over 50

min, resulting in 50% yield of the tetraphosphorylated K18 peptide at residues Ser 356, Tyr 310, Ser 262 and Ser 258 (Figure S13).

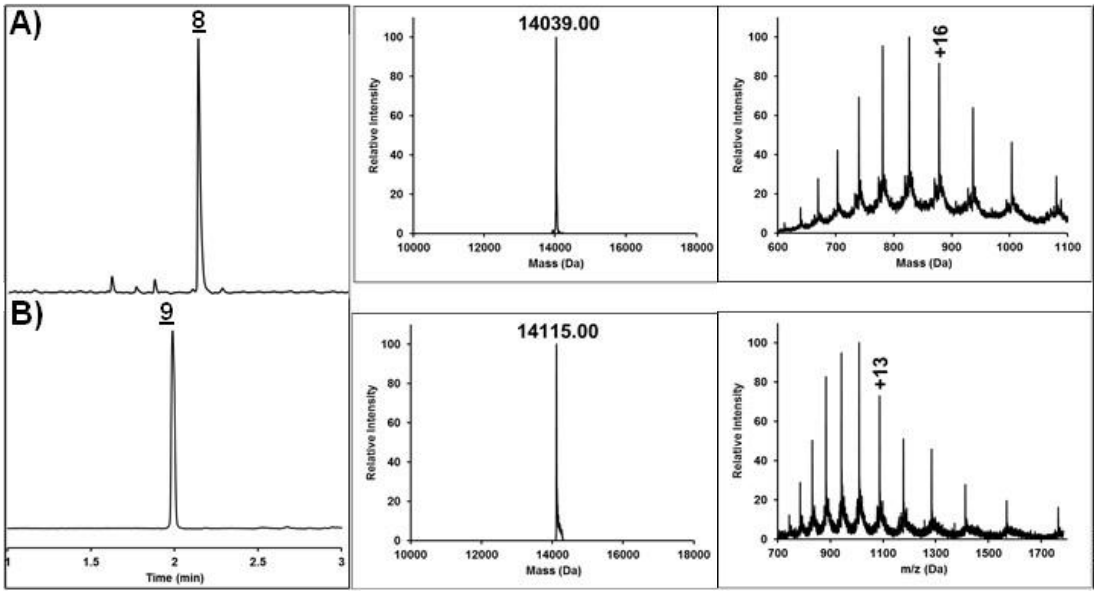

Figure S13. Analytical RP-HPLC and ESI-MS spectra of the *in vitro* phosphorylation reaction by c-Abl kinase at A) 0 h and after B) 5 h. Peak **9** corresponds to the tetraphosphorylated K18_pS356, pY310, pS262, pS258) with the observed mass of 14115.00 Da (calculated 14115.89 Da).

Circular dichroism (CD) measurements:

CD spectra were acquired on a Jasco J-815 CD spectrometer using a 1 mm quartz cuvette. Spectra were measured from 250 to 195 nm with a step size of 0.2 nm, a bandwidth of 1 nm, and a response time of 8 sec at 20 °C. For each spectrum, 5 scans were obtained and averaged. The averaged spectra were processed by smoothing using a binomial filter with a convolution width of 99 data points, and the resulting spectra were plotted as the mean residue molar ellipticity as a function of the wavelength.

***In vitro* aggregation studies:**

Lyophilized protein samples were dissolved in aggregation buffer (10 mM phosphate, 50 mM NaF, pH 7.4) to a final concentration of 10 μM. Protein concentrations were determined using a NanoDrop 1000 spectrophotometer operated at 280 nm. The pH was adjusted to 7.4 using 0.1 M NaOH, followed by filtration through 100 kDa molecular weight cutoff (MWCO) filters. Ten microliters of each K18 construct was incubated at 37

°C in the presence of heparin sodium salt (Applichem GmbH, Germany) at a 1:4 molar ratio (heparin:protein) supplemented with 10 μM of ThS (T1892 Sigma). The extent of fibrillization was measured in triplicate on a FLUOstar Omega® plate reader as a function of the ThS fluorescence (excitation wavelength: 440 nm, emission wavelength: 480 nm, cycle time: 10 min).

Transmission electron microscopy (TEM):

A total of 5 μL of each sample was deposited onto glow-discharged Formvar-coated 200 mesh copper grids (Electron Microscopy Sciences) for 90 sec. Grids were washed twice with dd H_2O, stained with 0.7% (w/v) uranyl formate for 30 sec and dried. A Tecnai Spirit BioTWIN electron microscope operated at 80 kV and equipped with a LaB_6 gun and a 4K × 4K FEI Eagle CCD camera was used to observe the samples and acquire the micrographs.

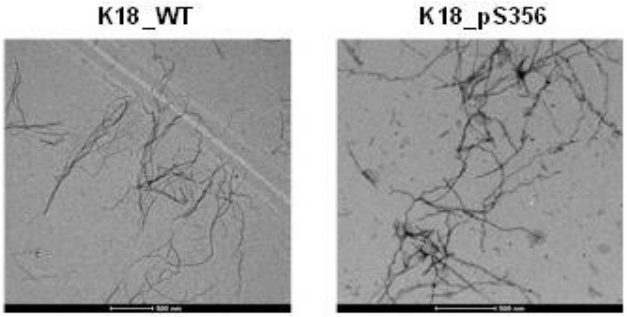

Figure S14. TEM images of WT and K18_pS356, after 48 h incubation at 37°C in the presence of heparin (scale bars are 500 nm).

Seeding assays:

Liposome-mediated transduction of tau seeds:

HEK293T tau biosensor cells stably express the tau repeat domain containing the disease-associated mutation (P301S), fused to cyan fluorescent protein (CFP) or yellow fluorescent protein (YFP). Cells were plated at 35,000 cells per well in a 96-well plate. After 18 h, the cells reached 60% confluency and were transduced with WT, mono-, di- and triphosphorylated K18 aggregate seeds at a final concentration of 100 nM (monomer equivalent) per well. Transduction complexes were prepared by combining [8.75 μL Opti-MEM (Gibco) +1.25 μL Lipofectamine 2000 (Invitrogen)] with [Opti-MEM + aggregate

seeds] for a total volume of 20 µL per well. Cells were incubated with the transduction complexes for 48 h to induce intracellular aggregation.

FRET flow cytometry:

Cells were harvested with 0.05% trypsin and fixed in 2% paraformaldehyde (Electron Microscopy Services) for 10 min, after which they were resuspended in flow cytometry buffer. A MACSQuant VYB (Miltenyi) was used to perform FRET flow cytometry. To measure CFP and FRET, cells were excited with a 405 nm laser, and fluorescence was captured with 405/50 nm (CFP) and 525/50 nm filters (FRET). To measure YFP, cells were excited with a 488 nm laser, and fluorescence was captured with a 525/50 nm filter. To quantify FRET, we used a gating strategy similar to that previously described. The integrated FRET density (IFD), defined as the percent of FRET-positive cells multiplied by the median fluorescence intensity of the FRET-positive cells, was used for all analyses. For each experiment, 20,000 cells were analyzed in quadruplicate. Analysis was performed using FlowJo v10 software (Treestar).

Seeding experiment 1:

K18 tau variants were incubated with or without heparin (Sigma) for a period of 24 h or 72 h at 25°C or 37°C. Samples were then used in the seeding assay at a final concentration of 100 nM (monomer equivalent) per well. Error bars represent the standard deviation.

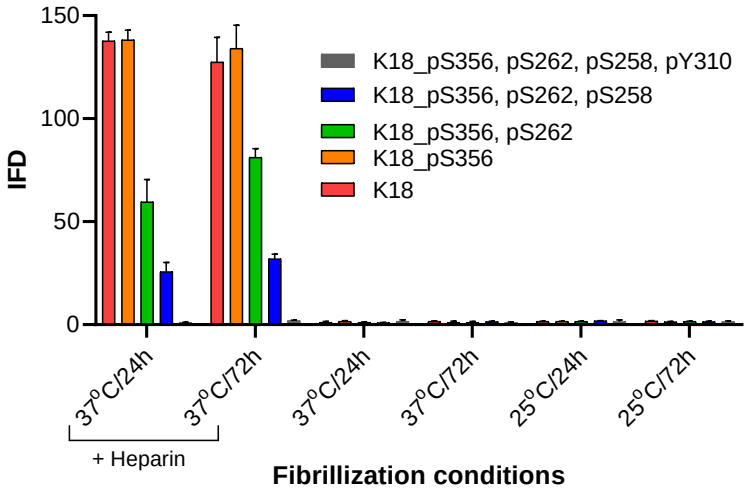

Figure S15. IFD measurements following the transduction of the WT, mono-, di- and triphosphorylated K18 previously incubated with or without heparin for various incubation times and temperatures.

Seeding experiment 2:

All constructs, except for K18_pS356, pS262, pS258, pY310, were incubated with heparin for various time periods (0, 30 min, and 1, 2, 3, 6, 12, 24 h) at 37°C. The samples were then frozen in liquid nitrogen and kept at -80°C. To quantify the seeding activity, samples were thawed on ice and tested immediately at 100 nM (monomer equivalent) per well. Error bars represent the standard deviation.

Seeding experiment 3:

K18 and K18_pS356 were incubated with heparin for various time periods (0, 1, 3, 5, 10, 15, 30, 45, 60 and 120 min) at 37°C. They were then frozen in liquid nitrogen and maintained at -80°C. To quantify the seeding activity, the samples were thawed on ice and tested immediately at 100 nM (monomer equivalent) per well. Error bars represent the standard deviation.

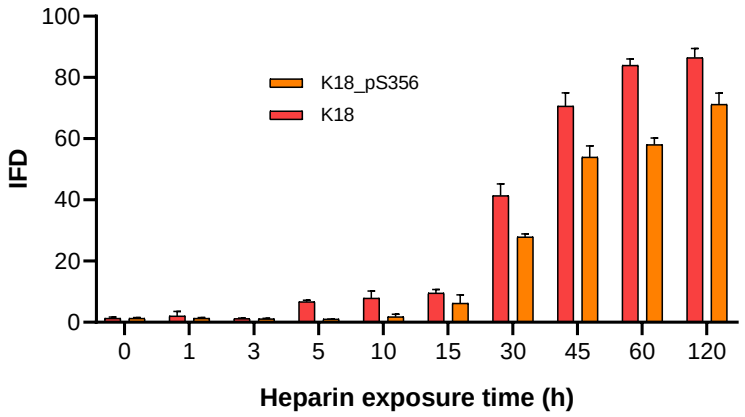

Figure S16. IFD measurements following the transduction of WT and pS356 K18 previously incubated at 37°C in the presence of heparin for various incubation times (0, 1, 3, 5, 10,15, 30, 45, 60 and 120 min).

Tubulin polymerization assay:

The tubulin assembly assay for K18 or the phosphorylated K18 (K18_pS356, K18_pS262, pS356, or K18_pS262, pS258, pS356) proteins was initiated by mixing 30 μM protein with tubulin (40 μM, in 100 μl total volume) in MT assembly buffer (80 mM PIPES pH 6.9, 2 mM $MgCl_2$ and 0.5 mM EGTA) supplemented with 1 mM GTP at 4 °C. The samples were

transferred and incubated in a water bath set at 37 °C for 4 min. Then, the polymerization was monitored by measuring the absorbance at 350 nm every 30 sec using a FLUOstar Omega plate reader incubated at 37 °C. Each experiment was performed in triplicate and repeated at least two times

Effect of phosphorylation on K18 proteins in Microtubule binding

To determine the binding of K18 proteins (K18, K18_pS356, K18_pS356, pS262 and K18_pS356, pS262, pS258) to microtubules, MT binding (sedimentation) assay was performed. Paclitaxel-stabilized MTs were used as a substrate to study the binding of the K18 proteins. The bound and non-bound K18 proteins to MTs were separated by ultra-centrifugation and the fractions were analysed through SDS PAGE to determine the

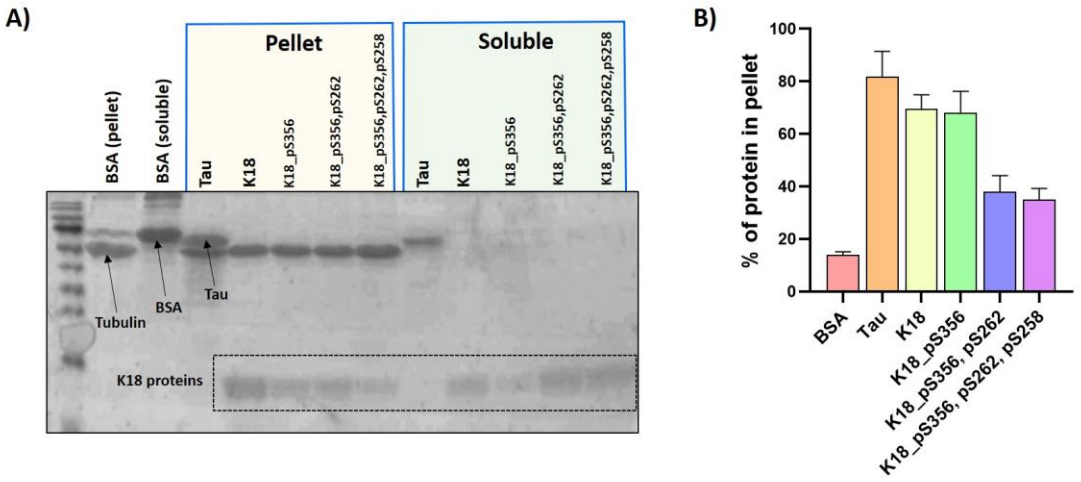

Figure S17. Phosphorylated K18 proteins binding to MTs. A) SDS PAGE showing K18, K18_pS356, K18_pS356, pS262 and K18_pS356, pS262, pS258 binding towards MTs. Tau was used as a positive control and BSA as a negative control. B) The binding of proteins to the MTs are quantified as the percentage of protein in the pellet when incubated with Paclitaxel stabilized MTs (200 µg/ml Tau and 200 µg/ml of tubulin). K18 (69%) and K18_pS356 (~67%) has higher binding towards MTs in comparison to K18_pS356, pS262 (37%) and K18_pS356, pS262, pS258 (35%). The positive control, Tau has a binding of ~80% towards MTs and negative control, BSA has ~14% binding towards MTs (4 repeats, represented as the mean ± SD).

percentage of K18 protein bound to MTs. As expected K18 (69%) showed higher binding towards MTs. Phosphorylation at S356 (K18_pS356, 67%) slightly decreases the binding of K18 to MTs. Whereas, K18_pS356, pS262 (37%) and K18_pS356, pS262, pS258 (37%) showed a significantly lower binding towards MTs. This observation is in good agreement with the tubulin polymerization assay (Figure 5). Tau (positive control) shows binding of ~80% and BSA (negative control) shows ~14% binding towards MTs. These attributes clearly indicate that phosphorylation at S262 and S256 significantly alter the MT binding.

Microtubules assembly and binding (sedimentation) assay[1]**:** The Tubulin protein was dissolved (10 mg/ml) in ice-cold tubulin buffer (80 mM PIPES, 0.5 mM EGTA, 2 mM $MgCl_2$, 1mM GTP and pH adjusted to 6.9, using KOH) and snap-frozen as 10 µl aliquots and stored at -80°C. 10 µl tubulin stock was thawed in a water bath at 37 ºC and immediately placed on ice. Then 1 uL of cushion buffer (tubulin buffer + 60 %glycerol) was added and incubated for 20 min at 37 °C in a pre-warmed (37 °C) water bath. Then 100 uL paclitaxel solution (100 uM) dissolved in tubulin buffer was added to stabilize the MTs. Paclitaxel-stabilized MTs were incubated for 60 min at RT with BSA, Tau, K18, K18_pS356, K18_pS356, pS262 and K18_pS356, pS262, pS258 (200 µg/ml protein and 200 µg/ml of tubulin). Each sample was placed on top of a 100 µl cushion buffer in 1.5 ml ultracentrifuge tubes. The samples were centrifuged at 100'000 g for 40 min at RT. The supernatant top 50 µl from each tube was mixed with 10 µl of 5x Laemmli buffer, the rest of the solution was carefully removed without disturbing the pellet and the pellet was resuspended in 50 µl 1x Laemmli buffer. The samples were run on SDS–PAGE gels and stained with instant blue. The relative amount of BSA, Tau, K18, K18_pS356, K18_pS356,

pS262 and K18_pS356, pS262, pS258 in the supernatant and in the pellet were estimated by measuring the band intensity using Fiji software (National Institute of Health) over 4 repeats, represented as the mean ± SD. The original image is converted to a 32bit image in ImageJ for better visibility and quantification.

Effect of phosphorylation on the structure and aggregation of K18

we reviewed the recent high-resolution atomic Cryo-EM structures of the tau filaments derived from the brains of patients with AD and Pick's disease.[2],[3] These structures revealed that tau filaments are composed of C-shaped subunits with resolved R3 and R4 repeat regions (306–378 residues) of the MTBD (Figure 6A). Interestingly, the high-resolution structure for the NPFs from Pick's disease patient exhibits different molecular

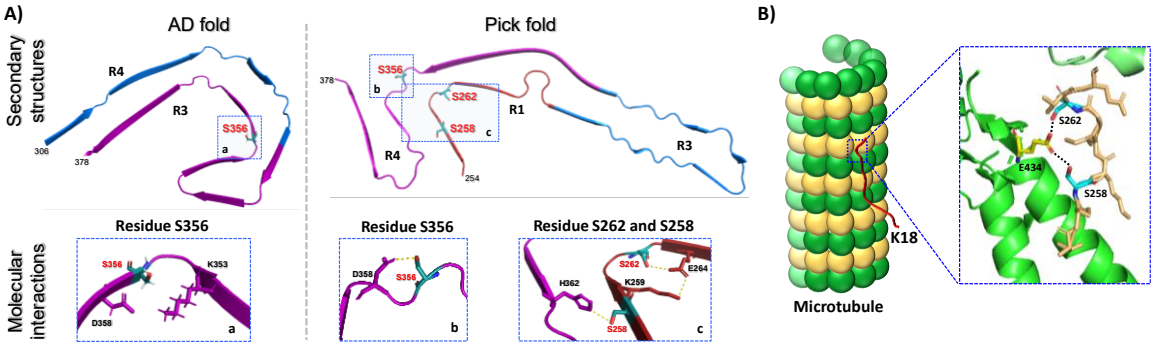

Figure S18. A) Rendered view of the secondary structure elements observed in Alzheimer's and Pick's filaments derived from the brains of AD and Pick's disease patients. The repeats R1, R3, and R4 of MTBD are highlighted in red, blue and purple, respectively. The polar interactions (hydrogen bonding) for the side chains of residues S356, S262 and S258 identified in AD and Pick's disease fold. B) Pictorial representation of the K18 fragment interacting with MT (left) and atomic model for the molecular interaction of pS258 and pS262 with E434 of the microtubule. The Cryo-EM structure reveals that S258, similar to S262, is in close proximity to MT and interacts with the E434 residue of MT, indicating possible roles of S258 and S262 in stabilizing the tau-MT complex.

interactions and conformations than the PHFs from AD patients. The minimal effect of phosphorylation at S356 on K18 fibrillization and seeding activity could be explained by the fact that the side chain of S356 does not participate in any major stabilizing interactions in either PHF. Similarly, in the context of the NPFs, S356 is not part of the sequence that constitutes the core of the filaments; it is located in the unstructured region (^{354}IGSLD^{358}) and does not seem to participate in major interactions with other key residues involved in stabilizing the filament formation. In contrast, the side chains of serine residues S262 and S258 exhibit spatial hydrogen bonding with adjacent AA residues in NFTs (Figure 6A). The S262 and S258 residues form hydrogen bonds with D264 and H362, respectively. Thus, phosphorylation of S262 would prevent the hydrogen bonding with E264 and significantly affect the molecular interaction between K259 and D264 through electrostatic repulsion. Similarly, phosphorylation of S258 would prevent hydrogen bonding with H362. These structural attributes clearly imply that phosphorylation at S262 and S258 could cause significant structural perturbations that could affect protein folding and aggregation. This could possibly explain the drastic decrease in the aggregation propensity of the di- (K18_pS356, K18_pS262) and tri- (K18_pS356, K18_pS262, K18_pS258) phosphorylated K18 proteins. The increase in the number of phosphorylation sites significantly perturbs key molecular interactions implicated in mediating pathological folding, leading to the complete inhibition of fibril formation. This clearly indicates the cumulative effect of the three phosphorylation sites on the inhibition of fibrillization. It is noteworthy that despite the fact that the R1 repeat is not part of the core of ex vivo filaments[4], several studies have consistently shown that sequence motifs within these region associated with disease-associated mutations[5], PTMs[6] or other sequence

perturbations significantly alter the kinetics and aggregation properties of tau. Our results show that phosphorylation within the MTBD inhibits tau fibril formation, which is contrary to the conventional wisdom that this enhances tau aggregation and fibrillization.

References

[1] C. Kesten, R. Schneider, S. Persson, *Bio-protocol* **2016**, *6*, e1759.

[2] A. W. P. Fitzpatrick, B. Falcon, S. He, A. G. Murzin, G. Murshudov, H. J. Garringer, R. A. Crowther, B. Ghetti, M. Goedert, S. H. W. Scheres, *Nature* **2017**, *547*, 185.

[3] B. Falcon, W. Zhang, A. G. Murzin, G. Murshudov, H. J. Garringer, R. Vidal, R. A. Crowther, B. Ghetti, S. H. W. Scheres, M. Goedert, *Nature* **2018**, *561*, 137–140.

[4] W. Zhang, B. Falcon, A. G. Murzin, J. Fan, R. A. Crowther, M. Goedert, S. H. W. Scheres, *Elife* **2019**, *8*, e43584.

[5] M. S. Wolfe, *J. Bio. Chem.* **2009**, *284*, 6021–6025.

[6] L. Martin, X. Latypova, F. Terro, *Neurochem. Int.* **2011**, *58*, 458–471.